United States
Environmental Protection
Agency

Robert S. Kerr Environmental
Research Laboratory
Ada, OK 74820

Research and Development

EPA/600/SR-94/018 March 1994

EPA

Project Summary

Abiotic Transformation of Carbon Tetrachloride at Mineral Surfaces

Michelle Kriegman-King and Martin Reinhard

Transformation of carbon tetrachloride (CCl_4) by biotite, vermiculite, and pyrite in the presence of hydrogen sulfide (HS^-) was studied under different environmental conditions. In systems containing biotite and vermiculite, the rate of CCl_4 transformation was dependent on the temperature, HS^- concentration, surface concentration, and Fe(II) content in the minerals. At 25°C, the half-life of CCl_4 with 1 mM HS^- was calculated to be 2600, 160, and 50 days for the homogeneous, vermiculite (114 m^2/L) and biotite (55.8 m^2/L) systems, respectively. The transformation rate with biotite and vermiculite was nearly independent of pH in the range 6-10 at constant HS^- concentration. The rate dependence on Fe(II) content of the sheet silicates suggested that the transformation occurs at surface sites where HS^- is associated with Fe(II).

CCl_4 reacted relatively rapidly in 1.2-1.4 m^2/L pyrite with >90% of the CCl_4 transformed within 12-36 days at 25°C. The observed rate law supports a heterogeneous reaction mechanism. The reactivity of CCl_4 with pyrite increased in the order: air-exposed pyrite/aerobic, air-exposed pyrite/HS^-, air-exposed pyrite/anaerobic, and acid-treated pyrite/anaerobic; but overall the reaction rate varied only by a factor of 2.5. The CCl_4 transformation products varied under different reaction conditions. In the sheet silicate systems, approximately 80-85% of the CCl_4 was transformed to CS_2 which hydrolyzed to CO_2; whereas only 5-15% of the CCl_4 was reduced to $CHCl_3$. In the pyrite systems, CO_2 was the major transformation product formed under aerobic conditions, whereas $CHCl_3$ was largely formed under anaerobic conditions. Formation of some CS_2 was observed in all pyrite systems.

This Project Summary was developed by EPA's Robert S. Kerr Environmental Research Laboratory, Ada, OK, to announce key findings of the research project that is fully documented in a separate report of the same title (see Project Report ordering information at back).

Introduction

The objectives of this research were to test the ability of ferrous iron-bearing minerals to abiotically transform carbon tetrachloride (CCl_4) in sulfidic (containing HS^-) environments. CCl_4 is a frequently found groundwater contaminant. The work focused largely on biotite, vermiculite, and pyrite as the ferrous iron-bearing minerals. Biotite and vermiculite are sheet silicates that are commonly found as detrital materials in sedimentary rocks. Sulfidogenic conditions are often observed in plumes of hazardous waste and landfill leachate. Specific factors that were studied include solid type and concentration, iron content, pH, temperature, sulfide concentration, CCl_4 concentration, and the presence or absence of oxygen. The CCl_4 transformation products were studied as a function of reaction conditions.

Procedure

Kinetic Studies

The base case reaction conditions to measure the disappearance rate of 1μ M CCl_4 in the biotite and vermiculite systems were pH = 7.5-8.5, temperature = 50°C, and [HS^-] = 1 mM. The solids concentrations for the base case were 55.8 m^2 biotite/L, and 114 m^2 vermiculite/L. Controls were established by reacting CCl_4

with HS^- at the same temperature and pH, but in the absence of the solids. Experiments with biotite were conducted over a pH range of 6-10, temperature range of 37.5-62.7°C, solids concentration of 11.2-280 m^2 biotite/L, and $[HS^-]$ = 0.02-4 mM. For all pyrite/CCl_4 transformation rate and product studies, 1 µM CCl_4 was reacted in aqueous systems containing 1.2-1.4 m^2/L pretreated pyrite at pH 6.5 and 25°C, except the experiments conducted with sulfide that were at pH 7.75. Experiments were conducted in a 1 mM NaCl ionic medium. Controls were established by reacting CCl_4 under the same conditions in the absence of pyrite in addition to reacting CCl_4 in homogeneous solutions of Fe^{2+}_{aq} or HS^-. For the studies of the pyrite oxidation products, 0.1-1 mM CCl_4 was reacted with large particles of pretreated pyrite (0.2 g). Controls were established by reacting pyrite under the same conditions but in the absence of CCl_4.

Materials

Biotite, vermiculite, muscovite, and pyrite were obtained from Ward's Scientific Establishment, Inc. (Rochester, NY). All transformation and adsorption studies were conducted in flame-sealed glass ampules because the reaction times were on the order of weeks to months, often at elevated temperature (50°C). Ampules were filled with approximately 13.5 mL of buffer that was filtered through a sterilized 0.2 µm nylon filter (Nalgene Corp., Rochester, NY).

Analytical Procedures

Reaction solutions were analyzed for CCl_4, $CHCl_3$, and CO using gas chromatography. Ion chromatography was used to measure formate and the potential pyrite oxidation products SO_3^{2-}, SO_4^{2-}, $S_2O_3^{2-}$. The CCl_4 product distribution was determined using ^{14}C-labeled substrate. Surfaces were characterized using XPS.

Mineral Characterization

Solids were characterized for specific surface area, [Fe(II)] and [Fe(III)]. XPS conducted on cleavage sheets of the biotite and vermiculite did not show the presence of any redox-sensitive trace metals besides iron. XPS studies indicated that sulfide does interact with the biotite surface, but the type and extent of effect sulfide has on the surface were not determined. The near surface S:Fe ratio of freshly cleaved pyrite was determined to be 2.1. After pyrite was reacted in aqueous solution under all reaction conditions, the near surface was depleted in iron with S:Fe>4. The oxidation state of the iron-depleted pyrite surface appeared unchanged when evaluated with XPS.

Equation	Number
$-\frac{d[CCl_4]}{dt} = k'_{obs}[CCl_4]^{\alpha} = (k'_{homo} + k'_{hetero})[CCl_4]^{\alpha}$	(1)
$= (k_{H_2O} + k'_{HS^-} + k'_{hetero})[CCl_4]^{\alpha}$	(2)
$= (k_{H_2O} + k_{HS^-}[HS^-]^{\beta 1}[H^+]^{\gamma 1} + k_{hetero}[HS^-]^{\beta 2}[H^+]^{\gamma 2}[SC]^{\delta})[CCl_4]^{\alpha}$	(3)
$k'_{obs} = k'_{CS_2} + k'_{CHCl_3} + k'_{NV}$	(4)
$[CS_2] = \frac{k'_{CS_2}[CCl_4]_0}{(k'_{obs} - k'_{CO_2})}[\exp(-k'_{CO_2} t) - \exp(-k'_{obs} t)]$	(5)
$[CO_2] = \frac{k'_{CS_2}[CCl_4]_0}{(k'_{obs} - k'_{CO_2})}[(1 - \exp(-k'_{CO_2} t)) - \frac{k'_{CO_2}}{k'_{obs}}(1 - \exp(-k'_{obs} t))]$	(6)
$[CHCl_3] = \frac{k'_{CHCl_3}[CCl_4]_0}{k'_{obs}}[1 - \exp(-k'_{obs} t)]$	(7)
$[Nonvol] = \frac{k'_{NV}[CCl_4]_0}{k'_{obs}}[1 - \exp(-k'_{obs} t)]$	(8)

Results and Discussion

Transformation of CCl_4 by Vermiculite and Biotite

Kinetic Modeling and Product Distributions

Observed pseudo-first-order rate constants (k'_{obs}) for the disappearance of CCl_4 in the vermiculite and biotite systems were calculated from regressions of $\ln([CCl_4]_t/[CCl_4]_0)$ vs. time where $[CCl_4]_0$ and $[CCl_4]_t$ were the CCl_4 concentrations at time = 0 and time = t, respectively. For experiments with k'_{obs}<0.001 day^{-1}, the transformation was considered negligible and was assumed to equal zero.

In the sheet silicates systems, the disappearance of CCl_4 was hypothesized to obey the laws shown in Equations 1 through 3, where α, $\beta 1$, $\beta 2$, $\gamma 1$, $\gamma 2$, and δ represent the reaction order with respect to reaction in solution and at the mineral interface, k'_{homo} and k'_{hetero} are pseudo-first-order rate constants, and k_{H_2O}, k_{HS^-} and k_{hetero} are intrinsic rate constants. Both the heterogeneous and homogeneous rate constants were first order with respect to $[CCl_4]$ (e.g. α = 1). The mineral surface area concentration (SC) was calculated from the product of the solids loading (g/L) and the specific surface area (m^2/g) of the mineral. The pK_a for the first dissociation of H_2S at the reaction temperature was used to calculate the HS^- concentration based on the pH and the amount of total sulfide added to the system. For homogeneous systems, $k'_{obs} = k'_{homo}$, where k'_{homo} accounts for the reactions with H_2O and HS^- in solution. In the heterogeneous systems, $k'_{hetero} = k'_{obs} - k'_{homo}$.

Rate constants for the different CCl_4 transformation pathways were evaluated by considering the relationship shown in Equation 4, where k'_{CS_2}, k'_{CHCl_3}, and k'_{NV} are pseudo-first-order rate constants that describe the formation of CS_2, $CHCl_3$, and the nonvolatile product, respectively. CO was detected in very small quantities and was not considered in this analysis. Data of CS_2, CO_2, $CHCl_3$ and nonvolatile concentrations as a function of time were fit to Equations 5, 6, 7, 8, respectively.

The rate constants, k'_{CS_2}, k'_{CO_2}, k'_{CHCl_3}, and k'_{NV} were estimated using both visual and nonlinear statistical curve-fitting. The rate constant k'_{CO_2} is the pseudo-first-order rate constant for the appearance of CO_2, due to CS_2 hydroly-

sis. The curve-fitting results for a typical experiment are shown in Figure 1. Good agreement was found across experiments in terms of the fraction of CCl_4 reacting via the three different pathways. A mass balance of 95-100% was obtained in these experiments.

At 50°C, pH 6-9, $SC_{biotite}$ = 0-280 m^2/L and low HS^- concentrations ($[HS^-]$<0.5 mM), the reaction orders from Equation 3 were determined to be $\alpha = 1$, $\beta 2 = 1.2$, and $\delta = 1$. The pH dependence in the environmentally relevant pH range was too low to be determined reliably and both $\gamma 1$ and $\gamma 2$ were assumed to be zero. At high HS^- concentrations ($[HS^-]$=0.5-4 mM) and $SC_{biotite}$<55.8 m^2/L, the rate of disappearance of CCl_4 in heterogeneous systems was independent of HS^- concentration ($\beta 2 = 0$).

The major transformation pathway of CCl_4 with HS^- is the formation of CO_2 via CS_2. It was proposed that CCl_4 undergoes reduction to form a trichloromethyl radical which then reacts with HS^-, S_x^{2-}, or $S_2O_3^{2-}$ to form CS_2 which hydrolyzes to CO_2. At 50°C, the rate constant for the disappearance of CS_2 ranged from 0.03 to 0.06 day^{-1}. Reported Arrhenius constants for the hydrolysis of CS_2 to CO_2 under reaction conditions herein, result in a hydrolysis rate of 0.006-0.015 day^{-1} at 25°C (half-life of 45-110 days). About 85% of the CCl_4 is ultimately transformed to CO_2 in these systems. Reductive dehalogenation of CCl_4 to $CHCl_3$ contributed to 5-15% of CCl_4 transformation. Ferrous iron in the sheet silicates appears to be playing a role in the transformation of CCl_4 with HS^-. It is most likely that the reaction is occurring at sites where HS^- is associated with ferrous iron.

Adsorption of CCl_4 onto biotite and vermiculite was determined by control experiments using radiolabeled CCl_4 at 25°C. Comparison of the aqueous CCl_4 concentration in the homogeneous and heterogeneous systems over four weeks showed less than 3% adsorption. Because the adsorption of CCl_4 was so small, CCl_4 measurements in the transformation studies were not corrected for adsorption.

The rate of hydrolysis (k_{H_2O}) of CCl_4 was calculated to be 0.002 day^{-1} at 50°C. In homogeneous systems, the CCl_4 transformation rate in the presence of sulfide is at least an order of magnitude greater than k_{H_2O} when $[HS^-]$>0.5 mM. In heterogeneous systems, the CCl_4 transformation rate is faster than k_{H_2O} with $[HS^-]$>0.05 mM and $SC_{biotite}$ = 55.8 m^2/L. The very low reactivity of HS^- in homogenous solution was enhanced in the presence of minerals indicating a catalytic effect of the surfaces.

Figure 1 depicts the disappearance of CCl_4, the appearance and disappearance of CS_2, and the appearance of products in a heterogeneous system (55.8 m^2/L biotite and 1 mM HS^-). About 65% of the CCl_4 was transformed to CO_2 after 60 days. At this time, approximately 20% of the CS_2 was remaining. Chloroform, formed via reductive dehalogenation of CCl_4, reached a maximum of 10%. $CHCl_3$ was shown to be relatively persistent in these systems when 5 µM $CHCl_3$ was reacted under the same conditions as the CCl_4 experiments. The half-life of $CHCl_3$ in the presence of 55.8 m^2/L biotite and 1 mM HS^- at 50°C was measured to be 172 days, whereas the half-life for hydrolysis of $CHCl_3$ at pH 7.75 and 50°C is 5000 days. Carbon monoxide and a nonvolatile component were measured as products in very small quantities (<5% combined) in the CCl_4 systems. The nonvolatile product, detected by ^{14}C fractionation measurements, was not identified in these systems.

Proposed Reaction Mechanism

The proposed chemical transformation pathways for CCl_4 under anaerobic conditions are summarized in Figure 2. The products and intermediates in the shadowed boxes were detected in our experiments. The first step for the transformation of CCl_4 has been proposed to be a one-electron reduction to form a trichloromethyl radical and Cl^-. This radical can follow several different pathways such as additional electron transfer to form a dichlorocarbene and Cl^-, dimerization to form hexachloroethane, or electron transfer and protonation to produce $CHCl_3$.

The only pathway previously suggested to form CO_2 under anaerobic conditions is

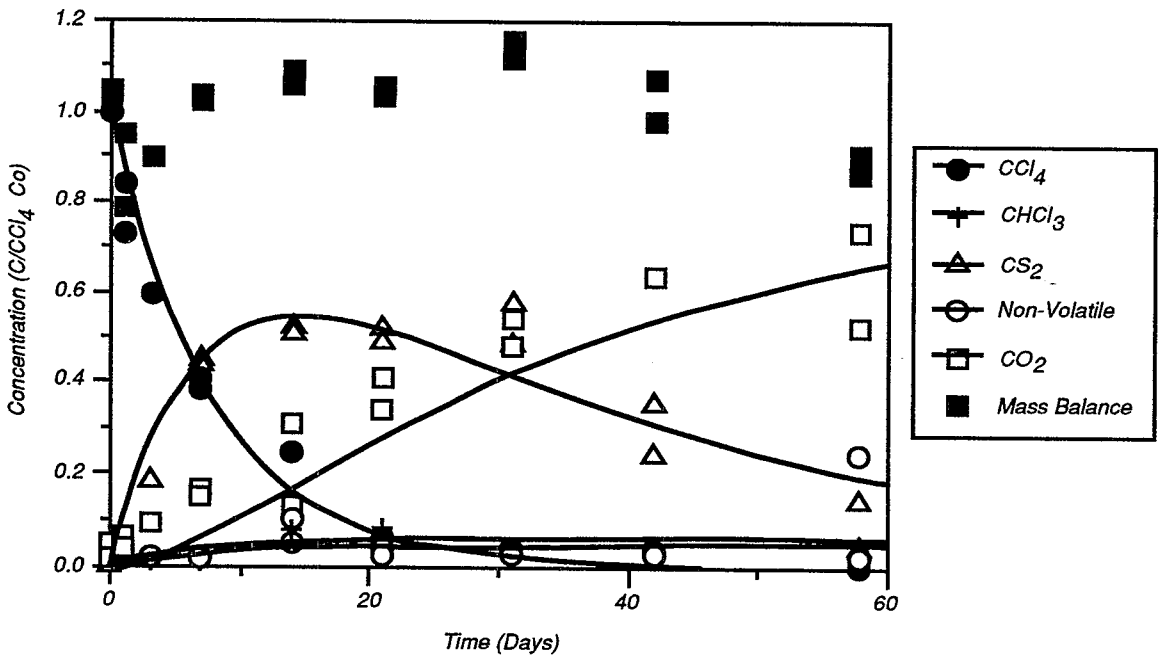

Figure 1. *CCl_4 transformation products from reaction with $[HS^-]$ = 1mM, $SC_{biotite}$ = 55.8 m^2/L, pH = 8.8 at 50°C.*

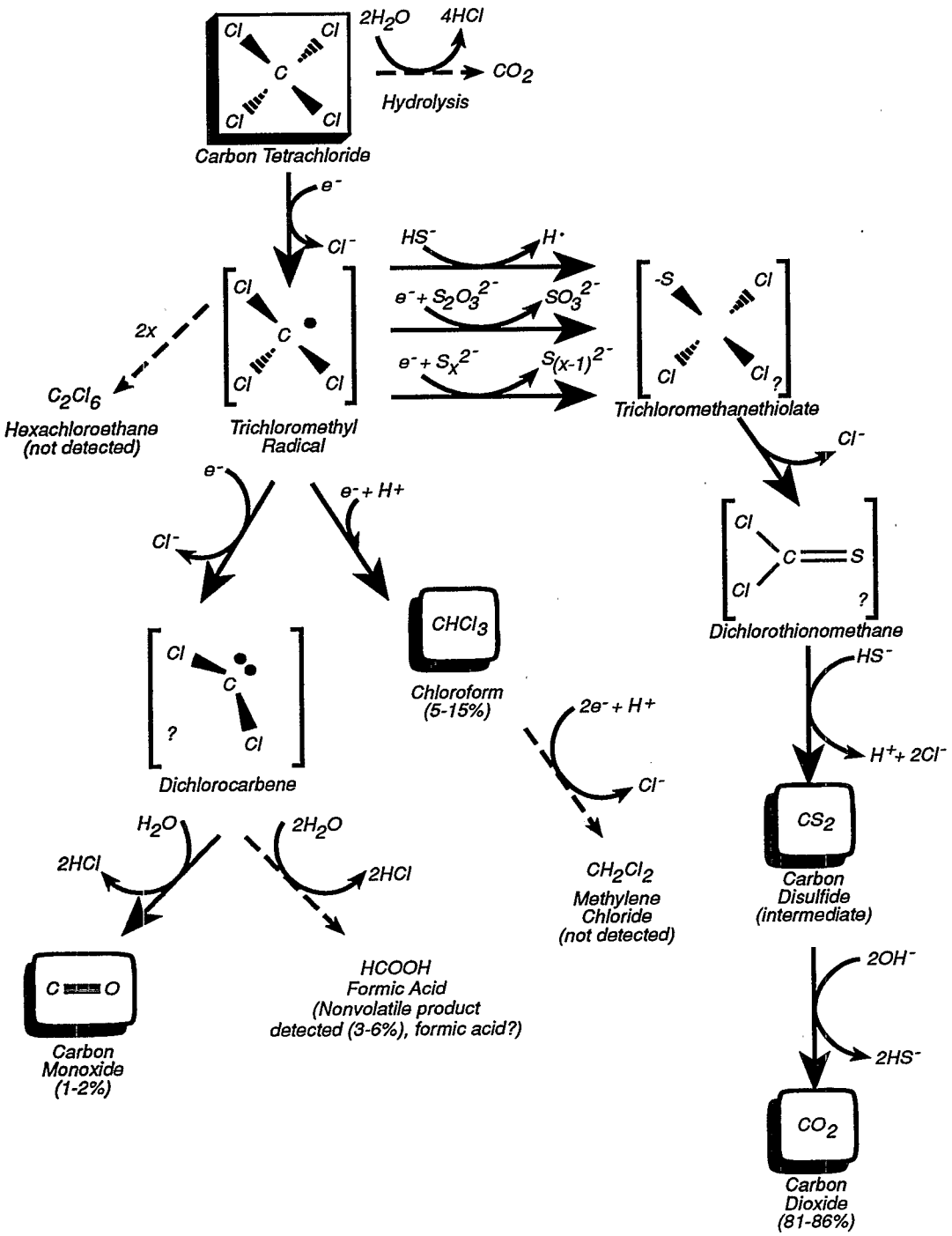

Figure 2. *Proposed CCl_4 transformation pathways in HS^- solution containing biotite. Compounds in shadowed boxes were detected in this study. Compounds in brackets are intermediates proposed in this study and from the literature (see Criddle and McCarty, 1991).*

direct hydrolysis (Criddle and McCarty, 1991). In our systems, CS_2 appears to be a major intermediate that is transformed to CO_2.

Temperature Dependence

From the temperature data collected at 37.5, 50.0, and 62.7°C, values for the Arrhenius activation energy (E_a) and pre-exponential (A) for the homogeneous, vermiculite, and biotite systems were calculated (Table 1). Lower E_a values in the heterogeneous systems indicate that these reactions will dominate the homogeneous reactions to an even greater extent at environmentally relevant temperatures. For example, at 50°C, CCl_4, in the presence of biotite and 1 mM HS^-, reacts 8 times faster than CCl_4 in the absence of biotite, whereas at 15°C, the biotite system reacts 125 times faster than the homogeneous system.

Table 1. *Arrhenius Parameters for CCl_4 Transformation with 1 mM HS^-: E_a and lnA Were Calculated Using $k'_{i,het}$ for Biotite and Vermiculite and k'_i for the Homogeneous Systems [a]*

System	E_a [kJ/mol]	ln(A) [ln(day^{-1})]
Homogeneous	122 ± 32 [b]	41.0 ± 2.1 [a]
Vermiculite	91.3 ± 8.4	31.4 ± 0.5
Biotite	59.9 ± 13.3	19.9 ± 0.9

[a] *Data collected at pH 7.5 and in the temperature range 37.5 - 62.7°C.*
[b] *95% confidence intervals.*

For the homogeneous reaction at 25°C, the half-life of CCl_4 with 1 mM HS^- was calculated to be 2600 days. In the presence of 1 mM HS^- and vermiculite (114 m^2/L) or biotite (55.8 m^2/L) 25°C, CCl_4 removal was first order with half-lives of 160 and 50 days, respectively. On a surface area normalized basis, CCl_4 transformation due to the presence of biotite was approximately six times greater than vermiculite.

Transformation of CCl_4 by Pyrite

Kinetic Modeling

The pyrite treatments and reaction conditions studied were as follows: air-exposed pyrite reacted aerobically, air-exposed pyrite reacted anaerobically, air-exposed pyrite reacted in the presence of sulfide, fresh-ground pyrite reacted anaerobically, and acid-treated pyrite reacted anaerobically. These conditions (except the acid treatment) were chosen to simulate different geochemical conditions. The data showed a much better adherence to zero-order model than to the first-order model. In the pyrite systems zero-order rate constants ($k^\circ_{CCl_4}$) were calculated from linear regressions of $[CCl_4]_t / [CCl_4]_0$ vs. time wherein $k^\circ_{CCl_4}$ is equal to -(slope)($[CCl_4]_0$). A poor fit was found for the fresh-ground system (R^2 = 0.65) presumably due to the heterogeneous nature of the freshly cleaved surfaces.

Rate constants for the disappearance of CCl_4 ($k^\circ_{CCl_4}$) are shown in Table 2. The rate constants were normalized by the pyrite surface concentration, assuming the reaction was first-order with respect to the surface concentration, SC, according to Equation 9.

In the acid-treated pyrite system, >90% of 1 μM CCl_4 was transformed within 12 days at 25°C, whereas half-lives in homogeneous solution are 1400 days for 1 mM HS^- at 25°C and 105 days for 0.1 mM Fe^{2+}_{aq} at 50°C. Assuming an activation energy of 60-120 kJ/mol, the half life of CCl_4 with 0.1 mM Fe^{2+}_{aq} at 25°C ranges from 700-4500 days. In Table 2, the data show that CCl_4 reacts the fastest with the acid-treated pyrite, although the air-exposed pyrite reacted anaerobically is not statistically slower. As expected, the slowest transformation rate was observed when CCl_4 was reacted with pyrite under aerobic conditions. However, the rate constant was only 2.5 times slower than the acid-treated system. The large error associated with the fresh-ground pyrite system precludes comparison with other rate constants. Reaction of air-exposed pyrite in the presence of sulfide shows that treatment of an oxidized pyrite surface with HS^- does not restore the reactivity of pyrite. Rather, sulfide appears to inhibit the transformation of CCl_4 by pyrite relative to the air-exposed/anaerobic pyrite system. At pH 7.75, 85% of the sulfide is present as HS^-; and more than 100 μM is present as H_2S. Because of the observed zero-order dependence on CCl_4, reaction sites on pyrite are inferred to be saturated with CCl_4 when $[CCl_4]$ = 1 μM. Additionally, since $[H_2S]$ was 100 times more concentrated than CCl_4 in these experiments, it is conceivable that H_2S blocks CCl_4 reaction sites. Characterization of the pyrite surface chemistry is necessary to understand the interaction of sulfide species with the pyrite surface.

CCl_4 Transformation Products

As shown in Table 3, the CCl_4 product distribution varies greatly depending on the reaction conditions even though $k^\circ_{CCl_4}$ only varies by a factor of 2.5. Under aerobic conditions, the major product was CO_2 (60-70%). Including the hydrolysis of CS_2 to CO_2, CO_2 accounts for 70-80% of the CCl_4 transformed. In contrast, the fresh-ground pyrite system forms approximately 50% $CHCl_3$ and ultimately only 10-20% CO_2. The total CO_2 amount in the fresh-ground system is a rough estimate because the speciation of the adsorbed fraction was not measured. Interestingly, some CS_2 was formed in all systems suggesting that the CCl_4 or reactive intermediates react with S_2^{2-} sites on pyrite, even in the presence of O_2. A fraction of the CCl_4 or its transformation products appeared to be adsorbed to pyrite.

The rate constants for the appearance of $CHCl_3$ and HCOOH (k'_{CHCl_3} and k°_{NV}, respectively) were evaluated assuming two

Table 2. *Zero-Order Rate Constants for CCl_4 Transformation with Pyrite (1.2-1.4 m^2/L) Reacted under Aerobic and Anaerobic Conditions at 25°C*

Pyrite Conditions	Slope (d^{-1})	R^2	$k^\circ_{CCl_4}$ ($mol/m^2 \cdot d$)	95% Confidence Interval
Air-exposed, Aerobic	0.025	0.93	0.021	0.017 - 0.026
Air-exposed, HS^-	0.031	0.87	0.026	0.020 - 0.032
Air-exposed, Anaerobic	0.057	0.85	0.047	0.035 - 0.049
Fresh-Ground	0.056	0.65	0.039	0.022 - 0.056
Acid-Pretreated	0.082	0.96	0.053	0.046 - 0.060

Equation	Number
$\frac{d[CTET]}{dt} = -k^\circ_{CCl_4}[SC]$	(9)

Table 3. CCl_4 Product Distribution in Percent from Reaction with Pyrite under Aerobic and Anaerobic Conditions at 25°C

Condition (Time in d)[a]	CCl_4	$CHCl_3$	CS_2	CO_2	Formate[b]	Adsorbed[c] NV + CO_2	Mass Balance[d]
Air-exposed; Aerobic (42)	0-1	5-6	11-15	52-59	2	10 (2 NV+ 8 CO_2)	84-87
Air-exposed, HS^- (31)	0-10	21-22	NM[e]	NM	NM	NM	NM
Air-exposed, Anaerobic (20)	0-1	28-30	0-3	26-30	7-9	12 (7NV + 5 CO_2)	82-84
Fresh-Ground (13)	1	48	2	10	5	12[f]	78
Acid-Pre-treated (13)	6-10	20-21	19-20	17	4	9 (2 NV + 7 CO_2)	78

[a] Reaction time in days is in parentheses.
[b] Formate was not directly measured. Formate was assumed to equal nonvolatile concentration.
[c] Adsorbed amount does not account for volatile compounds adsorbed. NV = nonvolatiles.
[d] Mass balance of aqueous volatile compounds was obtained in all cases. Total radioactivity in solution + adsorbed nonvolatile and CO_2 fractions are equal to the mass balance within 5%. Missing fraction likely to be adsorbed volatiles.
[e] NM = not measured.
[f] Breakdown of adsorbed products not measured.

Table 4. Rate Constants for the Disappearance of CCl_4 and Appearance of Intermediates and Products from Reaction with Pyrite under Aerobic and Anaerobic Conditions at 25°C

Rate Constant[a]		Air-exposed Pyrite Reacted Aerobically: No intermediate[b] $R^2_{adj} = 0.78$[d]	Air-exposed Pyrite Reacted Aerobically: Intermediate[c] $R^2_{adj} = 0.85$	Acid-treated Pyrite Reacted Aerobically: No intermediate[b] $R^2_{adj} = 0.85$	Acid-treated Pyrite Reacted Aerobically: Intermediate[c] $R^2_{adj} = 0.85$
$k^\circ_{CCl_4}$	[mol/m²·d]	0.021	0.021	0.053	0.053
k°_I	[mol/m²·d]	—	0.020	—	0.023
$k^\circ_{CS_2}$	[mol/m²·d]	0.0078	—	0.022	—
k'_{CS_2}	[L/m²·d]	—	0.012	—	7.7
k'_{CO_2}	[L/m²·d]	0.040	0.012	0.12	0.12
$k^\circ_{CHCl_3}$	[mol/m²·d]	0.00092	0.00092	0.012	0.012
k°_{NV}	[mol/m²·d]	0.00040	0.00040	0.0027	0.0027

[a] k° = zero-order rate constant; k' = first-order rate constant. For symbols see text.
[b] $CCl_4 \rightarrow CS_2 \rightarrow CO_2$.
[c] $CCl_4 \rightarrow Int \rightarrow CS_2 \rightarrow CO_2$.
[d] R^2_{adj} accounts for the number of fitting parameters.

Equation	Number
$\frac{d[CS_2]}{dt} = k^\circ_{CS_2} - k'_{CO_2}[CS_2]$	(10a)
$\frac{d[CO_2]}{dt} = k'_{CO_2}[CS_2]$	(10b)
$[CS_2] = \frac{k^\circ_{CS_2}}{k'_{CO_2}}\left(1 - \exp(-k'_{CO_2}t)\right)$	(11)
$\frac{d[Intermed.]}{dt} = k^\circ_I - k'_{CS_2}[Intermed.]$	(12)

different kinetic models (Table 4). Assuming CO_2 is formed only by the CS_2 pathway, Equations 10a and 10b can be used to solve for $[CS_2]$ and $[CO_2]$ as a function of time. In Equations 10a and 10b, $k^\circ_{CS_2}$ is a zero-order rate constant for the appearance of CS_2, and k'_{CO_2} is a first-order rate constant for the formation of CO_2.

The CS_2 data were fit with Equation 11 to solve for the rate constants, $k^\circ_{CS_2}$ and k'_{CO_2} (Table 4). These constants were then substituted into the equation for the formation of CO_2 to graphically verify the fit of the data. This model under-predicted CO_2 production, suggesting that CO_2 is formed via the reaction of CCl_3 with O_2. However, the curve for the appearance of CS_2 also did not fit the data well ($R^2_{adjusted} = 0.78$).

To model the time lag before the onset of the CS_2 increase, formation of a relatively stable intermediate in the path to form CS_2 was hypothesized. In this kinetic model, the appearance of CS_2 was modeled using Equations 12 and 13, where k°_I is the zero-order rate constant for the formation of the intermediate. In Equations 12 and 13, the rate constant for the appearance of CS_2 (k'_{CS_2}) is now assumed to be first order. The expression for the CS_2 concentration is shown in Equation 14.

The curve-fitting results are shown in Table 4 and Figure 3. At the end of the experiment, the model predicts that the intermediate attains a steady-state concentration of approximately 15% which agrees with the missing mass balance (Table 3).

A similar fitting analysis was conducted on the results from the acid-treated pyrite system. In this case, no significant difference in the CS_2 fit was observed if the

Equation	Number
$\frac{d[CS_2]}{dt} = k'_{CS_2}[Intermed.] - k'_{CO_2}[CS_2]$	(13)
$[CS_2] = \frac{k_I^\circ}{k'_{CO_2} - k'_{CS_2}} \left(\frac{k'_{CS_2}}{k'_{CO_2}} \exp(-k'_{CO_2} t) - \exp(-k'_{CS_2} t) \right) + \frac{k_I^\circ}{k'_{CO_2}}$	(14)
$\rangle FeS - S:^- + CCl_4 \rightarrow [\rangle FeS - S \cdot + CCl_4 \cdot^-] \rightarrow \rangle FeS - S - CCl_3 + Cl^-.$	(15)

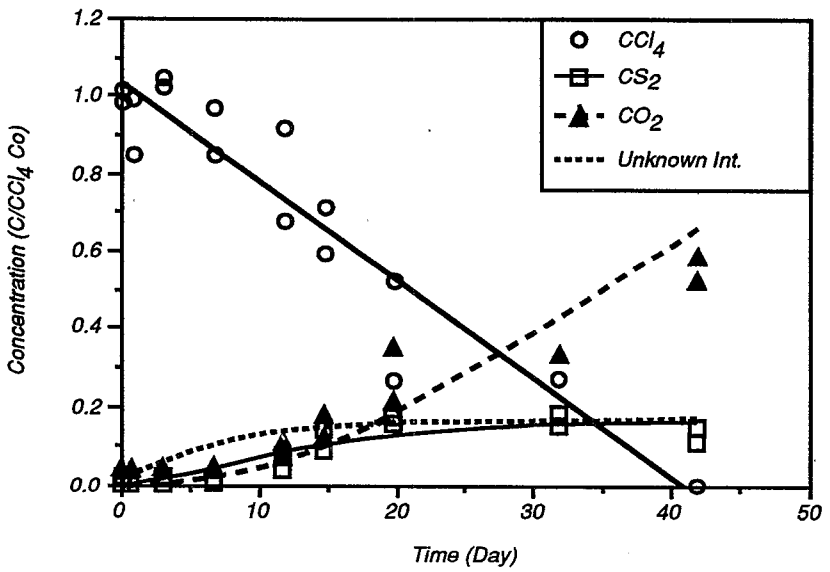

Figure 3. *Disappearance of CCl_4 in the presence of pyrite under aerobic conditions at 25°C. Appearance of the products, CS_2 and CO_2, with model results assuming the only path to form CO_2 from CCl_4 is: $CCl_4 \rightarrow$ Intermed. $\rightarrow CS_2 \rightarrow CO_2$.*

appearance of an unknown intermediate was included. As shown in Table 4, the rate constant for the disappearance of the unknown intermediate I (k_I°) was relatively large, indicating that the intermediate I is very short-lived. Therefore, k_I° is approximately equal to the rate constant for the appearance of CS_2 ($k^\circ_{CS_2}$).

Proposed Mechanism of CCl_4 Degradation at the Pyrite Surface

The proposed pathway of CCl_4 degradation by pyrite is summarized in Figure 4. Sulfur is the proposed electron transfer site in reactions of CCl_4 with pyrite because the surface was depleted in iron and CS_2 was detected under all reaction conditions. Since the pyrite surface was negatively charged under the reaction conditions in this study, the surface sites are proposed to be predominantly of the form >FeSS$^-$. It is assumed that the amphoteric nature of the leached pyrite surface is similar to that of pyrite-S. In the absence of oxidation of the pyrite surface, the electron transfer reaction with CCl_4 is proposed to occur via the reaction in Equation 15. The path to form CO_2 can occur via hydrolysis of CS_2 or reaction of the trichloromethyl radical with O_2. The former pathway is assumed to prevail under anaerobic conditions. However, under aerobic conditions, CO_2 is the major product in the pyrite system, and both pathways are possible.

Summary and Conclusions

The results of this work provide insight into the rates of CCl_4 transformation under different environmental conditions, the CCl_4 transformation products, and the mechanism of CCl_4 transformation at mineral surfaces. Major conclusions that can be drawn from this work include

(1) *The disappearance of CCl_4 in sulfidic systems was significantly faster in the presence of mineral surfaces (biotite, vermiculite, and pyrite) than in homogeneous solution.*

(2) *The rate of transformation of CCl_4 with the sheet silicates and sulfide depended on the following reaction conditions: temperature, surface concentration, sulfide concentration, and ferrous iron content in the minerals.* The CCl_4 transformation rate was investigated over the range of 6-10 at constant [HS$^-$]and showed a very shallow minimum at near-neutral pH.

(3) *The rate of transformation of CCl_4 with pyrite varied with reaction conditions in the following order: air-exposed pyrite/aerobic ≤ air-exposed pyrite/sulfide < air-exposed pyrite/anaerobic ≤ acid-treated pyrite/anaerobic.* The rate constants varied by only a factor of 2.5 for all the conditions studied. HS$^-$ inhibited the CCl_4 transformation rate by pyrite relative to systems reacted anaerobically in the absence of HS$^-$.

(4) *The CCl_4 transformation products varied greatly as a function of the reaction conditions.* In the sheet silicate/sulfide systems, CS_2 was identified as a major intermediate that hydrolyzed to CO_2, accounting for >85% of the CCl_4 transformed. In the pyrite systems, CS_2 was detected under all reaction conditions, suggesting that CCl_4 or an intermediate must react directly with the pyrite surface. Under aerobic conditions, CO_2 was the major transformation product (80%). In the fresh-ground pyrite systems, roughly 50% of the CCl_4 was transformed to $CHCl_3$. In all systems studied, formate and carbon monoxide were minor products.

(5) *The rate of transformation of CCl_4 with the sheet silicates was dependent on both the ferrous iron content and the sulfur concentration, indicating that the reaction occurs at sites where sulfide is associated with structural ferrous iron.*

(6) In the pyrite system, the near-surface was depleted of iron after reaction in water, while the oxidation state of the pyrite-S appeared to remain the same. *The high sulfur concentration at the near-surface makes it likely that*

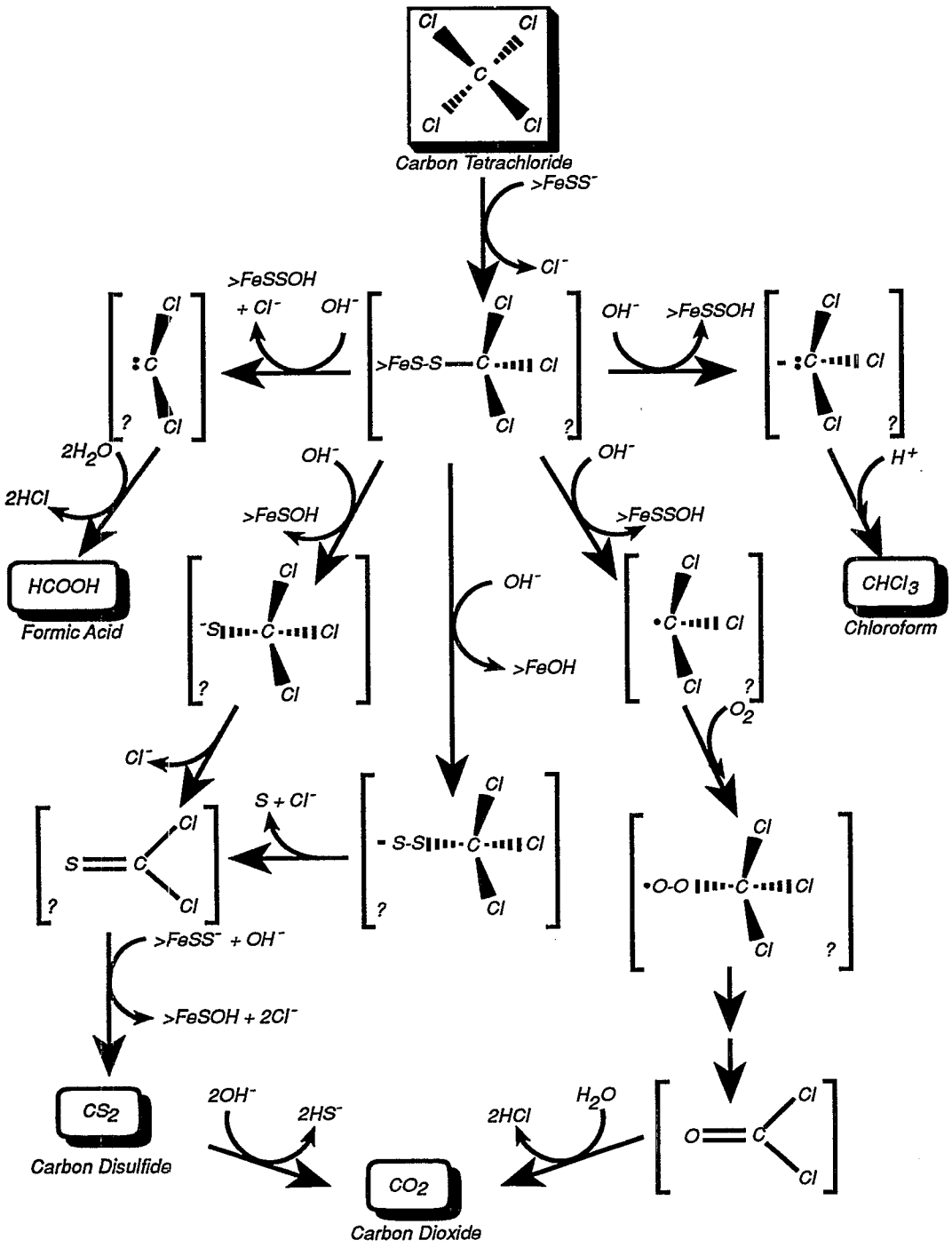

Figure 4. Proposed CCl_4 transformation pathways with pyrite. Compounds in shadowed boxes were measured. Compounds in brackets are proposed intermediates.

pyrite-S is the reductant of CCl_4, rather than pyrite-Fe.

Recommendations

The results of this study show that mineral surfaces may play a significant role in the fate of halogenated organics in the environment. Although they can be quantitatively applied to natural systems only with some difficulty, these data show that rate constants measured in deionized water will greatly under-predict the actual transformation rates. In pyrite- or sulfide-rich environments, abiotic transformation pathways may be significant on the time scale of groundwater transport. Predictive capabilities are complicated at this point due to the confounding effects of natural organic matter, cosolvents, competing oxidants, and microbial activity. To address these issues, continued research to further understand the surface chemistry of pyrite, the CCl_4 transformation pathway at the pyrite surface, and the reactivity of CCl_4 and other polyhalogenated aliphatics under field conditions is necessary. This work will ultimately lead to predictive capabilities.

The pyrite surface was relatively reactive with CCl_4 even under aerobic conditions; therefore, it is conceivable that a pyrite-based treatment system could be engineered. Further studies would have to be conducted in order to (1) identify the rate determining step of the reaction, (2) test the efficiency of the method in column and batch reactors, (3) control the CCl_4 product distribution, and (4) measure the pyrite oxidation products and ensure that they are harmless. In addition, the engineered system would have to be tested with other haloaliphatics to see if they could also be transformed and if they inhibited or effected the transformation of CCl_4

Reference

Criddle, C. S., and P. L. McCarty. 1991. Electrolytic model system for reductive dehalogenation in aqueous environments. *Environ. Sci. Technol.*, 25:973-978.

Michelle Kriegman-King and Martin Reinhard are with Stanford University, Stanford, California 94305-4020.
***Stephen R. Hutchins** is the EPA Project Officer (see below).*
The complete report, entitled "Abiotic Transformation of Carbon Tetrachloride at Mineral Surfaces," (Order No. PB94-144698; Cost: $19.50; subject to change) will be available only from
National Technical Information Service
5285 Port Royal Road
Springfield, VA 22161
Telephone: 703-487-4650
The EPA Project Officer can be contacted at
Robert S. Kerr Environmental Research Laboratory
U.S. Environmental Protection Agency
Ada, OK 74820

United States
Environmental Protection Agency
Center for Environmental Research Information
Cincinnati, OH 45268

Official Business
Penalty for Private Use
$300

EPA/600/SR-94/018

BULK RATE
POSTAGE & FEES PAID
EPA
PERMIT No. G-35